TECHNICAL NOTE:

CALCULATION OF EFFECTIVE GAS FLUX FROM SOIL FOLLOWING BAND APPLICATION OF MANURE OR FERTILIZER

T. R. Way, D. B. Watts, K. E. Smith, H. A. Torbert

ABSTRACT. *Greenhouse gases are emitted following application of manure and nitrogen-containing fertilizers to soil. Manure and fertilizers are often applied in subsurface bands in the soil, or in bands on the soil surface. This article presents a method that has been developed for calculating the effective gas flux for a multiple-band area to which manure or fertilizer has been applied in bands. The method has been developed for circular and rectangular flux chambers. In analyzing the method, a combination of CO_2 gas fluxes from a field experiment that gave a relatively low whole-plot effective flux and a combination that gave a relatively high whole-plot effective flux were used. For the lower-end flux situation, when the dimension of the flux chamber in the direction perpendicular to the band is considerably less than the band spacing, if the flux in a chamber that is centered on a band is assumed to be the whole-plot effective flux, then this assumption would overestimate the actual whole-plot effective flux by a considerable amount. The error of this type of assumption is reduced for the higher-end flux situation, regardless of flux chamber dimensions, and is reduced when the lower-end flux situation occurs and the dimension of the flux chamber in the direction perpendicular to the band is intermediate to nearly as large as the band spacing. The method in useful in calculating effective gas fluxes for whole plots to which manure or fertilizer has been band-applied.*

Keywords. Carbon dioxide, Emissions, Fertilizers, Greenhouse gases, Manures.

C oncerns about global warming have generated interest in evaluating the impacts of land use practices on greenhouse gas emissions. In the U.S., the annual CO_2 equivalent from agriculture is about 450 Tg of CO_2, based on about 40 Tg of CO_2 emitted from agriculture, about 280 Tg from N_2O emitted in crop and livestock production, about 170 Tg from CH_4 emitted from livestock production, and about -40 Tg from increased soil C storage (USEPA, 2008). Another negative consequence of greenhouse gas emissions from soil is the detrimental impact on soil quality from the loss of nitrogen and carbon from soil.

A variety of approaches have been used to determine CO_2 exchange fluxes between ecosystems and the atmosphere. These approaches include micrometeorological methods such as eddy covariance or gradient techniques used on towers or aircraft, diffusion modeling for bodies of water, and measurements using open (steady state) or closed (nonsteady state) chambers (Kutzbach et al., 2007). Probably the most widely used approach for measuring CO_2 efflux from bare soil surfaces is the closed chamber. The relatively small soil area covered by these chambers is well suited for the uneven soil surface found in many agricultural fields.

Two common methods that are used for applying manure and fertilizers to soil are broadcast application to the soil surface and subsurface band application. Gas flux chambers have often been used for determining fluxes from broadcast-applied fertilizers and manures, and have been used in some experiments to determine fluxes from band-applied fertilizers and manures. Mosier et al. (2006) and Halvorson et al. (2008) measured fluxes from soil in which manure or fertilizer had been applied in bands. They used rectangular flux chambers in a row crop experiment, and the chambers were placed perpendicular to the crop row, so the crop row and inter-row were contained within each chamber. Fertilizer treatments included subsurface band application of a urea-ammonium nitrate solution. Rectangular flux chambers (60 cm wide × 60 cm long) were used by Parkin (2008) to determine N_2O emissions directly over anhydrous ammonia fertilizer bands and midway between the fertilizer bands. The anhydrous ammonia was applied at a depth of 20 cm with a knife injector.

Determining gas fluxes from soil to which fertilizer or manure has been applied in bands is important, as it allows comparisons to be made with fluxes from broadcast application of fertilizer or manure. The objective of this article is to present a method for calculating gas fluxes that are representative of a whole plot, for band-applied manures or fertilizers, when the dimension of the flux chamber in the direction perpendicular to the length of the band is less than the band spacing, and when flux chambers are circular or rectangular in shape.

The method is useful for calculating effective fluxes for band-applied plots that have equally spaced bands. The effective flux here is the flux that is representative of the whole plot to which multiple bands have been applied. The method is appropriate for materials applied to soil in constant-width subsur-

The authors are **Thomas R. Way, ASABE Member Engineer,** Agricultural Engineer, and **Dexter B. Watts,** Soil Scientist, USDA-ARS National Soil Dynamics Laboratory, Auburn, Alabama; **Katy E. Smith,** Assistant Professor, Department of Math, Science, and Technology, University of Minnesota, Crookston, Minnesota; and **H. Allen Torbert,** Soil Scientist, USDA-ARS National Soil Dynamics Laboratory, Auburn, Alabama. **Corresponding author:** Thomas R. Way, USDA-ARS National Soil Dynamics Laboratory, 411 S. Donahue Dr., Auburn, AL 36832; phone: 334-844-4753; fax 334-887-8597; e-mail: tom.way@ars.usda.gov.

face bands and for materials applied in constant-width bands on the soil surface. The method can also be used when a material is subsurface-applied and the slot in the soil through which gases are likely to be emitted is of constant width.

For subsurface bands, this method is based on the assumption that gases emitted by the subsurface band of manure or fertilizer move vertically upward from the band and do not move laterally into the soil on each side of the band. Some gases likely move laterally from the band into the soil alongside the band and are emitted up through the surface of that soil, but this lateral flux away from the band is probably typically relatively small as a result of compaction of the soil walls of the trench formed when the band is applied.

Subsurface application of liquid manure in soil is typically done by injecting the slurry using a steel knife, sweep, or other soil-engaging device. Shape characteristics of manure-soil mix zones, as viewed along the implement direction of travel, were determined by Rahman et al. (2004, 2008). They showed that injection of liquid manure, or water mixed with dye, by a 330 mm width sweep or a 120 mm width custom-made injection tool resulted in relatively irregularly shaped manure-soil mix zones. The method presented here is based on the assumption that the band of manure or fertilizer has a constant width, so the method would not be appropriate for analysis of the irregularly shaped manure-soil mix zones described by Rahman et al. (2004, 2008), unless it can be assumed that gases emanate from only a constant-width portion of the soil surface, such as the slot formed by the injecting device.

Calculations that are more complex than the method presented here could be made. Such calculations could take into account the soil bulk density, soil air-filled porosity, soil water content, soil temperature, soil-gas diffusion coefficient, and other factors (Livingston et al., 2006; Venterea and Baker, 2008; Venterea et al., 2009). In addition, if Fick's laws are assumed to apply, then diffusive flux goes from regions of high concentration to regions of low concentration. The flux from the non-banded area within a chamber that is centered on a band is therefore likely to be suppressed as a result of the higher gas concentration in the chamber, as a consequence of the elevated flux from the banded region within the chamber. However, complexities of calculations that consider soil bulk
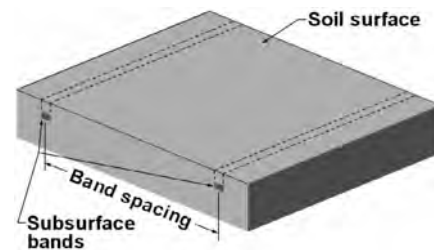

Figure 2. Soil in which two subsurface bands have been applied. Band spacing is the center-to-center spacing of the bands.

density and the other factors mentioned here, including the effects of Fick's laws, are beyond the scope of this article. Our objective here is to provide a simple calculation procedure that provides an estimate of the effective flux for a whole plot to which manure or fertilizer has been band-applied. Importantly, the method provides an estimate of the effective whole-plot flux.

DESCRIPTION OF THE METHOD

The method described here is useful for solid materials such as prilled fertilizer and broiler litter (fig. 1) and for liquid fertilizers, liquid animal slurries, and gaseous fertilizers such as anhydrous ammonia. Manure, fertilizer, or other material that is a potential emitter of gases is applied in subsurface bands (fig. 2) or bands on the soil surface. The bands are spaced at regular intervals. For example, poultry litter, which is a mixture of poultry manure and a bedding material such as pine shavings, peanut hulls, or rice hulls, may be applied in subsurface bands in a side-dressing application to a row crop, as described by Tewolde et al. (2009) and Farm Show (2009). The band spacing (fig. 2) for side-dressing of row crops is typically equal to the crop row spacing. In subsurface band application of poultry litter to a forage stand, typical subsurface band spacings of 25 to 38 cm have been used (Warren et al., 2008). Circular and rectangular flux chambers are commonly used (Parkin et al., 2003). Examples of the placement of the bases of flux chambers centered on subsurface bands for analysis of greenhouse gas fluxes are shown in figure 3.
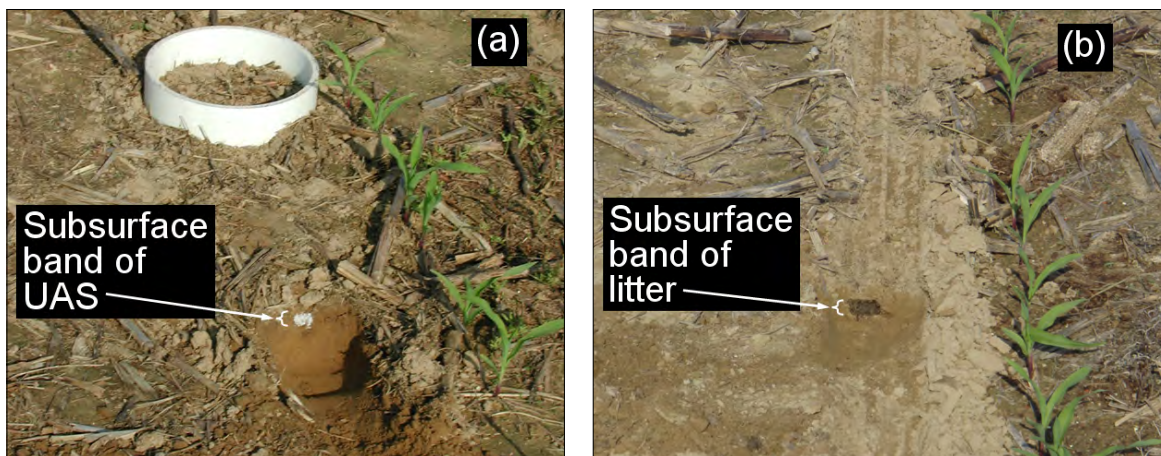

Figure 1. Subsurface bands of inorganic fertilizer and broiler litter. A small pit in the soil shows the cross-section of the band. (a) Subsurface band of prilled urea-ammonium sulfate (UAS) fertilizer that was side-dressed parallel to a corn (*Zea mays* L.) row. The base of the circular flux chamber (254 mm inside diameter) is centered over the band. (b) Subsurface band of broiler litter side-dressed parallel to a corn row. The broiler litter is a mixture of manure from broiler chickens (*Gallus gallus domesticus*) and a bedding material.
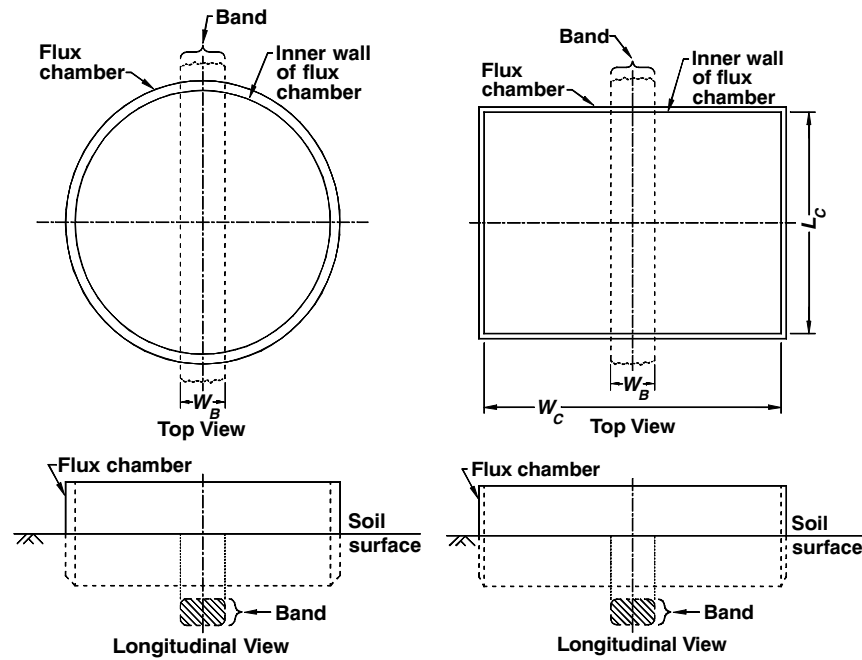
Figure 3. Top views and longitudinal views of a circular chamber and a rectangular chamber. Longitudinal view is the view in the direction of the band.

Flux chambers are commonly used in both pasture and row crop research. For pastures, the forage plants are typically present in both a chamber that is centered on a band and in a chamber that is in an untreated control area to which no manure or fertilizer has been applied. In row crops, we assume that the chamber that is centered on a band does not include a crop row because inclusion of a crop row in the chamber is beyond the scope of this method.

For visualizing gas fluxes, the fluxes may be represented by bars, in the sense of bar graphs, with the heights of the bars representing the flux values. The bar of height $F_{E,B}$ in figure 4 depicts a representative area of a banded plot, with $F_{E,B}$ being the soil surface effective gas flux for that area (variables are defined in the Nomenclature section). The dimension of the bar, in the direction perpendicular to the length of the band, is the band spacing, so the bar depicts an area that is representative of a plot that contains multiple bands. The flux ($F_{E,B}$) is the flux that we want to determine using the procedure presented here. The gas flux value from a circular flux chamber that is centered on a band ($F_{FC,B}$) is represented by the bar in figure 5. In this procedure, that flux value is assumed to be the weighted average of the flux from the band alone (F_B) and the flux from the non-banded area within the chamber (F_{NB}) (fig. 6).

The method presented here is based on the following two assumptions:

1. Any gas emitted from a subsurface band, and subsequently emitted from the soil surface, moves vertically straight up, so the gas does not diffuse horizontally into soil that is not directly above the band.
2. Changes in concentrations of gases in the chamber do not affect the fluxes from the banded and non-banded areas within the chamber.

Figure 5. Base of a circular flux chamber inserted into soil, centered on a subsurface band, so that the diameter of the base is collinear with the centerline of the band. The cylinder of height $F_{FC,B}$ represents the soil surface gas flux collected by the full chamber that is placed on the base. For clarity, the cylinder is shown separately from the base.
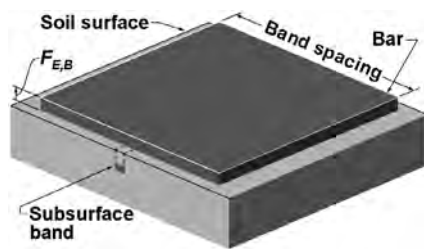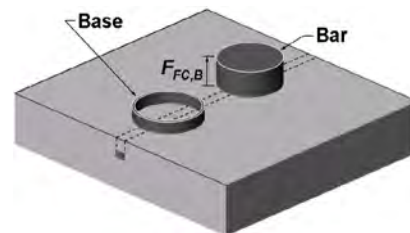

Figure 4. Bar graph representation of the soil surface effective gas flux for a banded plot ($F_{E,B}$). The bar is centered on the subsurface band. The bar width is equal to the band spacing because an area having a width equal to the band spacing is the minimum width for which $F_{E,B}$ is representative.
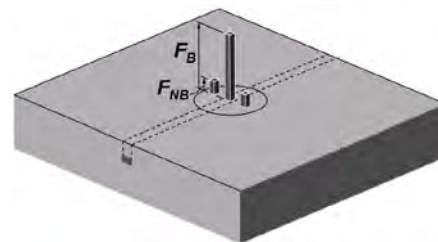

Figure 6. Bar graph representation of the breakdown of the soil surface gas flux for the full chamber that is centered on a band into its two constituent fluxes: F_B (soil surface gas flux for the band alone) and F_{NB} (soil surface gas flux for the non-banded area within the chamber). The circle on the soil surface represents the inner surface of the circular flux chamber.

The mass flow rate of a gas (e.g., μmol min⁻¹) into a fixed-volume element is the product of the gas flux (e.g., μmol m⁻² min⁻¹) and the area from which the gas emanates (e.g., m²). If two gases flow up through the soil surface into a flux chamber, then the product of the total mass flow rate of the gases into the chamber and the base area is equal to the sum of the product of the flux of the first gas and its portion of the base area and the product of the second gas and its portion of the base area (eq. 1):

$$F_{FC,B}\, A_C = F_B\, A_B + F_{NB}\, A_{NB} \qquad (1)$$

where $F_{FC,B}$ is the soil surface gas flux for a full chamber that is centered on a band (μmol m⁻² min⁻¹), F_B is the soil surface gas flux for the band alone (μmol m⁻² min⁻¹), F_{NB} is the soil surface gas flux for the non-banded area within the chamber (μmol m⁻² min⁻¹), A_C is the soil surface area within the chamber (m²), A_B is the horizontal area of the band within the chamber (m²), and A_{NB} is the soil surface area of the total non-banded portions within the chamber (m²).

The soil surface gas flux from a non-banded area, such as a control plot, is $F_{FC,Ctrl}$ (μmol m⁻² min⁻¹). From assumption 1 above, it follows that $F_{NB} = F_{FC,Ctrl}$. Using this substitution, equation 1 is solved for F_B:

$$F_B = (F_{FC,B}\, A_C - F_{FC,Ctrl}\, A_{NB})/A_B \qquad (2)$$

Importantly, in this method, within a flux chamber, the flux from the band (F_B) is not collected separately from the flux from the non-banded area (F_{NB}). Rather, the gas collected by a chamber that is centered on a band is a mixture of gas emitted from the band and from the non-banded area within the chamber. A chamber that is on an untreated control area is on an area of the soil surface to which no manure or fertilizer has been applied. The flux that is emitted into this chamber is $F_{FC,Ctrl}$. In the method, we do not measure F_B directly, but instead calculate it using equation 2.

Based on the flux and area relationships used in developing equation 1, equation 3 is developed here. If we consider a rectangular area of the soil surface that has its width equal to the band spacing, S_B (fig. 4), then the effective gas flux for that area is:

$$F_{E,B} = [F_B\, W_B + F_{FC,Ctrl}(S_B - W_B)]/S_B \qquad (3)$$

where $F_{E,B}$ is the soil surface effective gas flux for a banded plot (μmol m⁻² min⁻¹), S_B is the center-to-center band spacing (m), and W_B is the width of the band (m). Equations for calculating $F_{E,B}$ for circular and rectangular flux chambers are developed in the following sections.

CIRCULAR CHAMBER

A top view of a circular chamber that is centered on a band is shown in figure 7. The surface area of the band within the chamber is calculated from the area of the triangle and the area of the sector shown in figure 7:

$$A_B = 4(\text{area of one sector} + \text{area of one triangle}) \qquad (4)$$

where A_B is the surface area of the band within the flux chamber (m²). The angle θ, which is used in calculating the area of one sector (fig. 7) is:

$$\theta = \arcsin[(W_B/2)/R] \qquad (5)$$

where θ is the included angle of the sector of the circle (°), and R is the inside radius of the circular flux chamber (m).

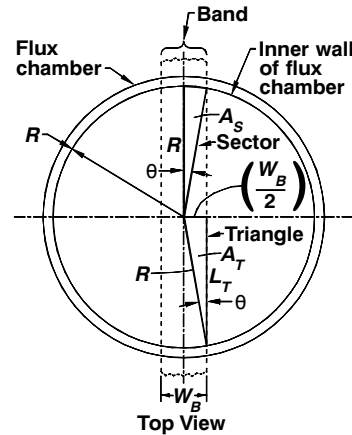Figure 7. Top view of circular flux chamber showing triangle and sector portions of the band.

The length of the longitudinal side of a triangle (L_T, m) is used in calculating the area of one triangle (fig. 7) and is:

$$L_T = \sqrt{R^2 - (W_B/2)^2} \qquad (6)$$

The area of one triangle (A_T, m²) is:

$$A_T = [(W_B/2) \times L_T]/2 \qquad (7)$$

The area of one sector (A_S, m²) is:

$$A_S = (\theta/360°) \times A_C \qquad (8)$$

For a circular flux chamber, the surface area within the chamber (A_C, m²) is:

$$A_C = \pi R^2 \qquad (9)$$

For flux chambers, whether circular or rectangular, the total surface area of the non-banded portions within the chamber (A_{NB}, m²) is:

$$A_{NB} = A_C - A_B \qquad (10)$$

RECTANGULAR CHAMBER

Calculations for a rectangular flux chamber are simpler because the geometry is simpler than for a circular chamber. The area of a band within a rectangular flux chamber (fig. 3) is:

$$A_B = W_B \times L_C \qquad (11)$$

where L_C is the inside length of the rectangular flux chamber in the direction parallel to the band (m) (fig. 3). For a rectangular flux chamber, the area within the chamber (A_C, m²) is:

$$A_C = L_C \times W_C \qquad (12)$$

where W_C is the inside width of the rectangular flux chamber in the direction perpendicular to the band (m). Three variables in the calculations for a rectangular flux chamber are determined using the same equations that are used for circular chambers: A_{NB} is calculated from equation 10, F_B is calculated from equation 2, and $F_{E,B}$ is calculated from equation 3.

NUMERICAL EXAMPLES

Numerical examples showing calculations for a circular chamber and a rectangular chamber are presented in the Appendix. Flux data used in the calculations are CO_2 flux data from the soil surface in a corn experiment conducted on a sandy loam soil at the Alabama Agricultural Experiment Sta-

tion's Sand Mountain Research and Extension Center at Crossville, Alabama. Broiler litter was applied in subsurface bands adjacent to the corn rows (fig. 1b) using the prototype implement developed at the USDA-ARS National Soil Dynamics Laboratory (Auburn, Ala.) for applying poultry litter in subsurface bands (Farm Show, 2009). The width of each subsurface band was assumed to be 44 mm, which was the trencher width on the implement. The USDA-ARS GRACEnet protocol allows CO_2 to be included as an analyte; however, when plants are present, interpretation of CO_2 data is complicated. In our experiment, the flux chambers did not contain any corn plants, weeds, or other plants, so no plants were present in the chambers, and interpretation of our CO_2 data was therefore uncomplicated. Each plot was 7.62 m (along the lengths of the corn rows) × 7.32 m, so the area of each plot was 55.7 m^2. The GRACEnet protocol recommends using as many flux chambers as possible and suggests a minimum of two chambers per treatment in plot-scale studies. The complete experiment had 96 plots (4 replications × 24 levels of treatment factors). Use of more than four replications would have exceeded the resources available for this experiment.

Samples of gas emitted from the soil surface were collected using *in situ* custom-made static gas flux chambers constructed according to the GRACEnet protocol (Parkin et al., 2003; Hutchinson and Mosier, 1981; Hutchinson and Livingston, 1993). The flux chambers were circular chambers constructed of 254 mm inside diameter (10 in. nominal diameter) schedule 40 PVC pipe. Base rings of the chambers were pressed into the soil, and just before gas sampling commenced, the upper portions of the chambers were placed on the base rings. Gas samples were taken at 0, 15, 30, and 45 min intervals following this chamber closure. This allowed the gas flux to be calculated from the change in concentration for the 45 min interval. At each time interval, gas samples (10 mL) were collected with polypropylene syringes and injected into evacuated glass vials (6 mL) fitted with butyl rubber stoppers, as described by Parkin and Kaspar (2006). The concentration of CO_2 was determined by comparison to a standard curve using standards obtained from Scott Specialty Gases (Plumsteadville, Pa.). The accuracy of the concentrations of these certified CO_2 standards is ±5%, as specified by the manufacturer. Gas fluxes were determined using the linear or curvilinear equations as appropriate, as di-

rected by the GRACEnet protocol (Parkin et al., 2003; Parkin and Kaspar, 2006). Gas samples were analyzed by a gas chromatograph (Shimadzu GC-2014, Columbia, Md.) equipped with a thermal conductivity detector for measuring CO_2.

A combination of mean flux data from the experiment that gave a relatively low effective gas flux for the banded plots ($F_{E,B}$) was a mean flux from chambers centered on the bands ($F_{FC,B}$) of 120 µmol m^{-2} min^{-1} along with a mean flux from chambers on control areas to which no manure or fertilizer had been applied ($F_{FC,Ctrl}$) of 40 µmol m^{-2} min^{-1}. Flux values for this situation are denoted here as "lower-end" values. These values are the means of four replications on one particular flux sampling day in conventional tillage plots. The combination of fluxes that gave a relatively high effective gas flux from the banded plots ($F_{E,B}$) was from no-till plots on a different day. That combination of fluxes was a mean flux from chambers centered on the bands ($F_{FC,B}$) of 300 µmol m^{-2} min^{-1} and a mean flux from chambers on control areas ($F_{FC,Ctrl}$) of 280 µmol m^{-2} min^{-1}. Flux values for this situation are denoted here as "higher-end" values. A Microsoft Excel spreadsheet for performing the calculations for circular chambers and rectangular chambers is available at "GF-Band" at www.ars.usda.gov/services/software/software. htm.

RESULTS
CIRCULAR CHAMBER

For a 0.76 m (30 in.) band spacing, which corresponds to a 0.76 m row spacing, the effective whole-plot flux calculated from the lower-end values (120 and 40 µmol m^{-2} min^{-1}) is 61.0 µmol m^{-2} min^{-1} (see Appendix and table 1) and that calculated from the higher-end values (300 and 280 µmol m^{-2} min^{-1}) is 285 µmol m^{-2} min^{-1} (table 1). When the row spacing, and hence the band spacing, is increased to 1.02 m (40 in.), the effective whole-plot flux calculated from the lower-end values is 55.8 µmol m^{-2} min^{-1} and that calculated from the higher-end values is 284 µmol m^{-2} min^{-1}.

For the example in which the lower-end flux values were used with the circular chamber and the 0.76 m band spacing, if the 120 µmol m^{-2} min^{-1} flux in the chamber that was centered on a band was assumed to be the whole-plot effective flux, then the assumption would overestimate the actual effective flux of 61.0 µmol m^{-2} min^{-1} by 97% (table 1). In the

Table 1. Whole-plot effective fluxes, fluxes from chambers centered on bands, and errors that occur when
the effective flux from the whole plot is assumed to be the flux from a chamber centered on a band.

	Circular Chamber (254 mm inside diameter)				Rectangular Chamber (60 cm × 40 cm)[a]				Rectangular Chamber (25 cm × 40 cm)[b]			
	0.76 m Band Spacing		1.02 m Band Spacing		0.76 m Band Spacing		1.02 m Band Spacing		0.76 m Band Spacing		1.02 m Band Spacing	
	Lower end[c]	Higher end	Lower end	Higher end	Lower end	Higher end	Lower end	Higher end	Lower end	Higher end	Lower end	Higher end
Whole-plot effective flux (µmol m^{-2} min^{-1})												
	61.0	285	55.8	284	61.0	285	55.8	284	61.0	285	55.8	284
Flux from chamber centered on band (µmol m^{-2} min^{-1})												
	120	300	120	300	66.7	287	66.7	287	104	296	104	296
Error (%)[d]	97	5	115	6	9	1	20	1	70	4	86	4

[a] Chamber dimensions are 60 cm in the direction perpendicular to the band by 40 cm in the direction parallel to the band.
[b] Chamber dimensions are 25 cm in the direction perpendicular to the band by 40 cm in the direction parallel to the band.
[c] "Lower end" denotes flux values that gave relatively low effective whole-plot fluxes, and
"higher end" denotes flux values that gave relatively high effective whole-plot fluxes.
[d] Error = (Flux from chamber centered on band - Whole-plot effective flux) / Whole-plot effective flux × 100.

similar example with the 1.02 m band spacing, if the 120 μmol m^{-2} min^{-1} flux in the chamber that was centered on a band was assumed to be the whole-plot effective flux, the assumption would overestimate the actual effective flux of 55.8 μmol m^{-2} min^{-1} by 115%. For the higher-end flux values, the differences between the whole-plot effective flux and the on-band chamber flux are considerably less. In the example for which the higher-end flux values were used with the circular chamber and the 0.76 m band spacing, if the 300 μmol m^{-2} min^{-1} flux in the chamber that was centered on a band was assumed to be the whole-plot effective flux, the assumption would overestimate the actual effective flux of 285 μmol m^{-2} min^{-1} by 5%. In the higher-end flux example with the 1.02 m band spacing, if the 300 μmol m^{-2} min^{-1} flux in the chamber that was centered on a band was assumed to be the whole-plot effective flux, the assumption would overestimate the actual effective flux of 284 μmol m^{-2} min^{-1} by 6%.

RECTANGULAR CHAMBER

Calculations for the circular chambers show that the soil surface gas flux for a band alone (F_B) is 405 μmol m^{-2} min^{-1} for the lower-end flux values (see Appendix) and 371 μmol m^{-2} min^{-1} for the higher-end flux values. Here, we use these values to examine characteristics of a rectangular flux chamber measuring 60 cm in the direction perpendicular to the band and 40 cm in the direction parallel to the band. The band spacing is 0.76 m, and the band width is 44 mm. For the F_B value of 405 μmol m^{-2} min^{-1} and the corresponding control flux ($F_{FC,Ctrl}$) of 40 μmol m^{-2} min^{-1}, the flux from the chamber centered on the band ($F_{FC,B}$) is calculated using equation 1 and solved for $F_{FC,B}$ to be 66.7 μmol m^{-2} min^{-1}. As described in the Appendix, the whole-plot effective flux is calculated from F_B, $F_{FC,Ctrl}$, the band width, and the band spacing, so for the rectangular chamber with the lower-end flux scenario, the whole-plot effective flux is 61.0 μmol m^{-2} min^{-1}, the same as the value for the lower-end situation for the circular chamber. If the 66.7 μmol m^{-2} min^{-1} flux from this rectangular chamber centered on a band was assumed to be the whole-plot effective flux, the assumption would overestimate the actual effective flux of 61.0 μmol m^{-2} min^{-1} by 9% (table 1). For the higher-end flux scenario with the rectangular chamber and the 0.76 m band spacing, the effective whole-plot flux is 285 μmol m^{-2} min^{-1}. If the 287 μmol m^{-2} min^{-1} flux from this rectangular chamber centered on a band (table 1) was assumed to be the whole-plot effective flux, the assumption would overestimate the actual effective flux of 285 μmol m^{-2} min^{-1} by only 1%.

For the same rectangular chamber and a band spacing of 1.02 m, for the lower-end flux situation, if the 66.7 μmol m^{-2} min^{-1} flux from the chamber centered on a band (table 1) was assumed to be the whole-plot effective flux, the assumption would overestimate the actual effective flux of 55.8 μmol m^{-2} min^{-1} by 20%. For the higher-end flux scenario, if the 287 μmol m^{-2} min^{-1} flux from this rectangular chamber centered on a band (table 1) was assumed to be the whole-plot effective flux, the assumption would overestimate the actual effective flux of 284 μmol m^{-2} min^{-1} by only 1%.

These errors for the 60 cm × 40 cm rectangular chamber are considerably less than the corresponding errors for the 254 mm diameter circular chamber. This is a result of the relatively large 60 cm dimension of this rectangular chamber in the direction perpendicular to the band, compared to the 254 mm maximum dimension of the circular chamber in the

direction perpendicular to the band. As illustrated in table 1, a rectangular chamber that has a relatively narrow 25 cm dimension in the direction perpendicular to the band and this same 40 cm in the direction parallel to the band, has relatively large error values for the lower-end flux situation, compared to error values for the 60 cm × 40 cm chamber.

For given values of soil surface gas flux for a band alone (F_B) and flux from a chamber on a control area to which no manure or fertilizer has been applied ($F_{FC,Ctrl}$), calculation of the whole-plot effective flux ($F_{E,B}$) is not affected by the diameter of the circular chamber (see Appendix). In addition, as described in the Appendix, for given values of F_B and $F_{FC,Ctrl}$ when a rectangular chamber is used, calculation of the whole-plot effective flux is not affected by the chamber dimension in the direction perpendicular to the band.

The method presented here provides calculations of effective gas fluxes of whole plots to which manure or fertilizer has been band-applied. Importantly, when the dimension of a flux chamber in the direction perpendicular to the length of the band is less than the band spacing, this method should be used for calculating the whole-plot effective gas flux. Validation of the calculation method, for example by collecting whole-plot gas flux, is beyond the scope of this article, so we did not attempt to validate the method. Rather, this article presents the calculation method and numerical examples based on representative soil gas fluxes.

The gas flux calculation method presented here is useful for band application of manure or fertilizer for any band spacing greater than the inside diameter of a circular flux chamber or the corresponding inside dimension of a rectangular flux chamber. The method is useful for band applications in both row crops and pastures.

CONCLUSIONS

A method for calculating gas fluxes that are representative of a whole plot, for band-applied manures or fertilizers, was presented. The method is useful when the dimension of a flux chamber in the direction perpendicular to the band is less than the band spacing and when flux chambers are circular or rectangular in shape. In analyzing the method, a combination of CO_2 gas fluxes from a field experiment that gave a relatively low whole-plot effective flux and a combination that gave a relatively high whole-plot effective flux were used. For the lower-end flux situation, when the dimension of the flux chamber in the direction perpendicular to the band is considerably less than the band spacing, if the flux in a chamber that is centered on a band is assumed to be the whole-plot effective flux, this assumption would overestimate the actual whole-plot effective flux by a considerable amount. The error of this type of assumption is reduced for the higher-end flux situation, regardless of the flux chamber dimensions, and is reduced for the lower-end flux situation when the dimension of the flux chamber in the direction perpendicular to the band is intermediate to nearly as large as the band spacing. The method is useful in calculating effective gas fluxes for whole plots to which manure or fertilizer has been band-applied.

REFERENCES

Farm Show. 2009. Prototype applicator buries poultry litter. *Farm Show* 33(2): 25. Lakeville, Minn.: Farm Show Publishing.

Halvorson, A. D., S. J. Del Grosso, and C. A. Reule. 2008. Nitrogen, tillage, and crop rotation effects on nitrous oxide emissions from irrigated cropping systems. *J. Environ. Qual.* 37(4): 1337-1344.

Hutchinson, G. L., and G. P. Livingston. 1993. Use of chamber systems to measure trace gas fluxes. In *Agricultural Ecosystem Effects on Trace Gas and Global Climate Change*, 63-78. L. A. Harper, A. R. Mosier, J. M. Duxbury, and D. E. Rolston, eds. ASA Special Publication 55. Madison, Wisc.: ASA.

Hutchinson, G. L., and A. R. Mosier. 1981. Improved soil cover method for field measurements of nitrous oxide fluxes. *SSSA J.* 45(2): 311-316.

Kutzbach L., J. Schneider, T. Sachs, M. Giebels, H. Nykänen, N. J. Shurpali, P. J. Martikainen, J. Alm, and M. Wilmking. 2007. CO_2 flux determination by closed-chamber methods can be seriously biased by inappropriate application of linear regression. *Biogeosci.* 4(6): 1005-1025.

Livingston, G. P., G. L. Hutchinson, and K. Spartalian. 2006. Trace gas emission in chambers: A non-steady-state diffusion model. *SSSA J.* 70(5): 1459-1469.

Mosier, A. R., A. D. Halvorson, C. A. Reule, and X. J. Liu. 2006. Net global warming potential and greenhouse gas intensity in irrigated cropping systems in northeastern Colorado. *J. Environ. Qual.* 35(4): 1584-1598.

Parkin, T. B. 2008. Effect of sampling frequency on estimates of cumulative nitrous oxide emissions. *J. Environ. Qual.* 37(4): 1390-1395.

Parkin, T. B., and T. C. Kaspar. 2006. Nitrous oxide emissions from corn-soybean systems in the Midwest. *J. Environ. Qual.* 35(4): 1496-1506.

Parkin, T. B., A. R. Mosier, J. L. Smith, R. T. Venterea, J. M. F. Johnson, D. C. Reicosky, G. Doyle, G. W. McCarty, and J. M. Baker. 2003. USDA-ARS GRACEnet chamber-based trace gas flux measurement protocol. Beltsville, Md.: USDA-ARS. Available at: www.ars.usda.gov/SP2UserFiles/person/31831/2003GRACEnetTraceGasProtocol.pdf. Accessed 24 November 2010.

Rahman, S., Y. Chen, K. Buckley, and W. Akinremi. 2004. Slurry distribution in soil as influenced by slurry application micro-rate and injection tool type. *Biosystems Eng.* 89(4): 495-504.

Rahman, S., Y. Chen, J. Paliwal, and B. Assefa. 2008. Models for manure distribution in soil following liquid manure injection. *Trans. ASABE* 51(3): 873-879.

Tewolde, H., S. Armstrong, T. R. Way, D. E. Rowe, and K. R. Sistani. 2009. Cotton response to poultry litter applied by subsurface banding relative to surface broadcasting. *SSSA J.* 73(2): 384-389.

USEPA. 2008. Inventory of U.S. greenhouse gas emissions and sinks: 1990-2006. EPA 430-R-08-005. Washington, D.C.: U.S. EPA Office of Atmospheric Programs.

Venterea, R. T., and J. M. Baker. 2008. Effects of soil physical nonuniformity on chamber-based gas flux estimates. *SSSA J.* 72(5): 1410-1417.

Venterea, R. T., K. A. Spokas, and J. M. Baker. 2009. Accuracy and precision analysis of chamber-based nitrous oxide gas flux estimates. *SSSA J.* 73(4): 1087-1093.

Warren, J. G., K. R. Sistani, T. R. Way, D. A. Mays, and D. H. Pote. 2008. A new method of poultry litter application to perennial pasture: Subsurface banding. *SSSA J.* 72(6): 1831-1837.

NOMENCLATURE

A_B horizontal area of band within a flux chamber (m^2)

A_C soil surface area within a flux chamber (m^2)

A_{NB} soil surface area of the total non-banded portions within a flux chamber that is centered on a band (m^2)

A_S area of sector of circle within a circular flux chamber (fig. 7) (m^2)

A_T area of triangle within a circular flux chamber (fig. 7) (m^2)

F_B soil surface gas flux for a band alone ($\mu mol\ m^{-2}\ min^{-1}$)

$F_{E,B}$ soil surface effective gas flux for a banded plot ($\mu mol\ m^{-2}\ min^{-1}$)

$F_{FC,Ctrl}$ soil surface gas flux for a control plot ($\mu mol\ m^{-2}\ min^{-1}$)

$F_{FC,B}$ soil surface gas flux for a full chamber that is centered on a band ($\mu mol\ m^{-2}\ min^{-1}$)

F_{NB} soil surface gas flux for the non-banded area within a chamber that is centered on a band ($\mu mol\ m^{-2}\ min^{-1}$)

L_C inside length of a rectangular flux chamber in the direction parallel to the band (fig. 3) (m)

L_T length of side of triangle that is parallel to the length of the band in a circular flux chamber (m)

S_B band spacing (center-to-center) (m)

R inside radius of circular flux chamber (m)

W_C inside width of a rectangular flux chamber in the direction perpendicular to the band (fig. 3) (m)

W_B width of band (m)

θ included angle of sector of circle (fig. 7) (°)

APPENDIX: NUMERICAL EXAMPLES

CIRCULAR FLUX CHAMBER

In this example, a circular flux chamber is made from 254 mm inside diameter (10 in. nominal diameter) schedule 40 PVC pipe.

Width of band:

$$W_B = 0.044\ m$$

Band spacing (center to center):

$$S_B = 0.762\ m$$

Soil surface gas flux for a control plot:

$$F_{FC,Ctrl} = 40\ \mu mol\ m^{-2}\ min^{-1}$$

Soil surface gas flux for full chamber that is centered on a band:

$$F_{FC,B} = 120\ \mu mol\ m^{-2}\ min^{-1}$$

Solution

Inside radius of circular chamber:

$$R = 0.127\ m$$

Length of side of triangle in circular flux chamber:

$$L_T = \sqrt{R^2 - (W_B/2)^2}$$

$$= \sqrt{(0.127\ m)^2 - (0.044\ m/2)^2}$$

$$= 0.12508\ m$$

Area of triangle:

$$A_T = \left[(W_B/2) \times L_T\right]/2$$

$$= \left[(0.044\,\text{m}/2) \times 0.12508\,\text{m}\right]/2$$

$$= 0.0013759\ \text{m}^2$$

Included angle of sector of circle:

$$\theta = \arcsin\left[(W_B/2)/R\right]$$

$$= \arcsin\left[(0.044\,\text{m}/2)/0.127\,\text{m}\right]$$

$$= 9.976°$$

Soil surface area within circular chamber:

$$A_C = \pi R^2 = \pi (0.127\,\text{m})^2$$

$$= 0.050671\ \text{m}^2$$

Area of sector of circle within circular chamber:

$$A_S = (\theta/360°) \times A_C$$

$$= (9.976°/360°)(0.050671\,\text{m}^2)$$

$$= 0.0014041\ \text{m}^2$$

Horizontal area of band portion that is bounded by the inner wall of the flux chamber:

$$A_B = 4(\text{area of one triangle} + \text{area of one sector})$$

$$= 4(0.0013759\,\text{m}^2 + 0.0014041\,\text{m}^2)$$

$$= 0.011120\ \text{m}^2$$

Area of non-banded soil surface within flux chamber:

$$A_{NB} = A_C - A_B$$

$$= (0.050671 - 0.011120)\,\text{m}^2$$

$$= 0.039551\ \text{m}^2$$

Soil surface gas flux for a band alone:

$$F_B = (F_{FC,B}A_C - F_{FC,Ctrl}A_{NB})/A_B$$

$$= \left[(120\,\mu\text{mol m}^{-2}\,\text{min}^{-1})(0.050671\,\text{m}^2)\right.$$

$$\left. - (40\,\mu\text{mol m}^{-2}\,\text{min}^{-1})(0.039551\,\text{m}^2)\right]$$

$$\div\,0.011120\ \text{m}^2$$

$$= 404.5\ \mu\text{mol m}^{-2}\,\text{min}^{-1}$$

Soil surface effective gas flux for a banded plot:

$$F_{E,B} = \left[F_B W_B + F_{FC,Ctrl}(S_B - W_B)\right]/S_B$$

$$= \left[(404.5\,\mu\text{mol m}^{-2}\,\text{min}^{-1})(0.044\,\text{m})\right.$$

$$\left. + (40\,\mu\text{mol m}^{-2}\,\text{min}^{-1})(0.762\,\text{m} - 0.044\,\text{m})\right]$$

$$\div\,0.762\ \text{m}$$

$$= 61.0\ \mu\text{mol m}^{-2}\,\text{min}^{-1}$$

Whole-Plot Effective Flux is Independent of Flux Chamber Diameter

As described above, for the lower-end flux situation, for a circular chamber with an inside diameter of 254 mm, a band spacing of 0.76 m, a band width of 44 mm, $F_{FC,B} = 120$ μmol m^{-2} min^{-1}, and $F_{FC,Ctrl} = 40$ μmol m^{-2} min^{-1}, the soil surface gas flux for a band alone (F_B) is 404.5 μmol m^{-2} min^{-1}, and the whole-plot effective flux ($F_{E,B}$) is 61.0 μmol m^{-2} min^{-1}. Using $F_B = 404.5$ μmol m^{-2} min^{-1}, $F_{FC,Ctrl} = 40$ μmol m^{-2} min^{-1}, a band spacing of 0.76 m, and a band width of 44 mm, with a chamber inside diameter of 203 mm (8 in.), the whole-plot effective flux ($F_{E,B}$) is calculated as 61.0 μmol m^{-2} min^{-1}, which is the equal to the value from the 254 mm inside diameter chamber. Therefore, the whole-plot effective flux is independent of flux chamber diameter.

Rectangular Flux Chamber

In this example, the inside dimensions of a rectangular chamber are 60 cm × 40 cm. For the chamber that is centered on a band, the 60 cm width of the chamber is perpendicular to the band.

Inside width of the rectangular flux chamber:

$$W_C = 0.60\ \text{m}$$

Inside length of the rectangular flux chamber:

$$L_C = 0.40\ \text{m}$$

Width of band:

$$W_B = 0.044\ \text{m}$$

Band spacing (center to center):

$$S_B = 0.762\ \text{m}$$

Soil surface gas flux for a control plot:

$$F_{FC,Ctrl} = 40\ \mu\text{mol m}^{-2}\,\text{min}^{-1}$$

Soil surface gas flux for full chamber that is centered on a band:

$$F_{FC,B} = 66.73\ \mu\text{mol m}^{-2}\,\text{min}^{-1}$$

To make this example similar to the lower-end flux situation with a 0.76 m band spacing described in the Rectangular Chamber part of the Results section, $F_{FC,B}$ here is 66.73 μmol m^{-2} min^{-1}.

Solution

Soil surface area within the chamber:

$$A_C = L_C \times W_C$$

$$= (0.40\,\text{m})(0.60\,\text{m})$$

$$= 0.2400\ \text{m}^2$$

Horizontal area of band portion that is bounded by the inner wall of the flux chamber:

$$A_B = W_B \times L_C$$

$$= (0.044\,\text{m})(0.40\,\text{m})$$

$$= 0.01760\ \text{m}^2$$

Area of non-banded soil surface within flux chamber:

$$A_{NB} = A_C - A_B$$

$$= (0.2400 - 0.01760) \text{ m}^2$$

$$= 0.2224 \text{ m}^2$$

Soil surface gas flux for a band alone:

$$F_B = (F_{FC,B}A_C - F_{FC,Ctrl}A_{NB})/A_B$$

$$= [(66.73 \, \mu\text{mol m}^{-2} \text{ min}^{-1})(0.2400 \text{ m}^2)$$

$$- (40 \, \mu\text{mol m}^{-2} \text{ min}^{-1})(0.2224 \text{ m}^2)]$$

$$\div 0.01760 \text{ m}^2$$

$$= 404.5 \, \mu\text{mol m}^{-2} \text{ min}^{-1}$$

Soil surface effective gas flux for a banded plot:

$$F_{E,B} = [F_B W_B + F_{FC,Ctrl}(S_B - W_B)]/S_B$$

$$= [(404.5 \, \mu\text{mol m}^{-2} \text{ min}^{-1})(0.044 \text{ m})$$

$$+ (40 \, \mu\text{mol m}^{-2} \text{ min}^{-1})(0.762 \text{ m} - 0.044 \text{ m})]$$

$$\div 0.762 \text{ m}$$

$$= 61.0 \, \mu\text{mol m}^{-2} \text{ min}^{-1}$$

Whole-Plot Effective Flux is Independent of Flux Chamber Dimension in the Direction Perpendicular to the Band

Here we first consider the lower-end flux situation with a rectangular chamber measuring 60 cm in the direction perpendicular to the band and 40 cm in the direction parallel to the band. The band spacing is 0.76 m, and the band width is 44 mm. As described above, for the F_B value of 404.5 μmol m^{-2} min^{-1} and the corresponding control flux ($F_{FC,Ctrl}$) of 40 μmol m^{-2} min^{-1}, the flux from the chamber centered on the band ($F_{FC,B}$) is 66.7 μmol m^{-2} min^{-1} and the whole-plot effective flux ($F_{E,B}$) is 61.0 μmol m^{-2} min^{-1}. Next we consider a similar situation, but with the chamber dimension in the direction perpendicular to the band now being 40 cm. The following are still true: this is the lower-end flux situation, the band spacing is 0.76 m, the band width is 44 mm, F_B = 404.5 μmol m^{-2} min^{-1}, and $F_{FC,Ctrl}$, = 40 μmol m^{-2} min^{-1}. The whole-plot effective flux ($F_{E,B}$) is 61.0 μmol m^{-2} min^{-1}, which is the equal to the value from the rectangular chamber measuring 60 cm in the direction perpendicular to the band. Therefore, the whole-plot effective flux is independent of the flux chamber dimension in the direction perpendicular to the band.